Galvanic corrosion of aluminium–copper model alloys

Jonathan Idrac [a], Georges Mankowski [a], George Thompson [b], Peter Skeldon [b], Yolande Kihn [c], Christine Blanc [a,*,1]

[a] *CIRIMAT, UMR CNRS 5085, ENSIACET, 118 route de Narbonne, 31077 Toulouse Cedex 04, France*
[b] *Corrosion and Protection Centre, UMIST, Manchester M60 1QD, UK*
[c] *CEMES/CNRS, BP 4347, 31055 Toulouse Cedex 4, France*

Abstract

Galvanic coupling between different α and θ phase-containing model Al–Cu alloys, deposited by magnetron sputtering, has revealed that the anodic α phase did not suffer corrosion and remained in the passive state in sulphate solution. Conversely, sulphate ions induced pitting of the cathodic θ phase. Pitting susceptibility of the cathode increased when the difference between the copper content of the anode and cathode increased. Similar observations were made for all the galvanic couples; further, the higher the copper content of a phase, then the greater its susceptibility to pitting.

Keywords: Aluminium; Copper; Intermetallics; Galvanic coupling; Sulphate

1. Introduction

In commercial aluminium–copper alloys, the various alloying elements result in the presence of different metallurgical phases in the matrix, including strengthening particles, dispersoids and coarse intermetallic particles [1–4]. In the AA2024 alloy for instance, two types of intermetallic particle, AlCuMg and AlCuMnFe, are generally found. These particles, which can vary in size up to a few tens of microns, occupy about 2–4% of the total surface area. The Al–Cu–Mg particles (i.e. Al_2CuMg particles) contain on average 38 wt.% Cu and 16 wt.% Mg, and the AlCuMnFe particles contain about 27 wt.% Cu, 11 wt.% Fe and 6 wt.% Mn [3]. The chemical compositions can vary significantly from particle to particle and even within the particles [5]. When aluminium–copper alloys are immersed in a corrosive environment, a complex electrochemical behaviour can be generated due to differences in reactivities of the various phases, leading to galvanic coupling between them [6–8]. The zones surrounding the particles, which have modified chemical compositions compared with the matrix, resulting from a depletion of alloying elements, can also participate in the galvanic coupling. Further, the corrosion behaviour of such alloys obviously depends on the chemical composition of the media since species such as chlorides are aggressive towards the matrix and the copper-rich particles, whereas sulphates, which can also be aggressive to copper-rich intermetallic particles, have an inhibitive effect on the corrosion of the aluminium matrix [9,10].

For such alloys, it is difficult to analyse the effects of the different galvanic couples. Thus, many authors have used micrometer-scale electrochemical techniques, but these techniques are often expensive and difficult to use [7,8,11,12]. Moreover, because of the significant variation in the chemical composition of coarse copper-rich intermetallics, a statistical analysis is required; this is difficult to perform with micrometer scale approaches. A further possibility is to study the galvanic coupling between different model aluminium–copper alloys which allows simplification of the system [13,14]. Hence, this paper is devoted to further understanding of the influence of copper content on the galvanic coupling current measured when two binary Al–Cu alloys, containing 0.2–100 at.% Cu, are connected.

2. Experimental

Binary Al–Cu alloys, containing 0.2–100 at.% Cu, were deposited using an Atom Tech Ltd magnetron sputtering sys-

* Corresponding author. Tel.: +33 5 62 88 57 08; fax: +33 5 62 88 56 63.
E-mail address: Christine.Blanc@ensiacet.fr (C. Blanc).
[1] ISE member.

doi:10.1016/j.electacta.2007.05.056

tem, using separate high purity aluminium (99.999%) and copper (99.99%) targets. The alloys were deposited on substrates consisting of electropolished 99.99% aluminium foils. The deposition chamber was first evacuated to 4×10^{-7} mbar, with sputtering then carried out at 5×10^{-3} mbar in 99.998% argon at 300 K. The deposition rate was about 9 nm min^{-1} and the total alloy layer thickness was in the approximate range of 400–500 nm.

Suitable electron transparent sections, prepared by ultramicrotomy, of freshly deposited alloys were examined by transmission electron microscopy (TEM) using a Tecnai F30 G2 microscope, operating at an accelerating voltage of 300 kV.

Galvanic coupling tests consisted of recording the current flow with time resulting from coupling of two aluminium–copper alloys of different copper contents. The tests were performed in 0.1 M Na_2SO_4 solution at room temperature for 2 h, using similar exposed surface areas for the two electrodes (2 cm^2).

The different alloys are termed "Al–*x*Cu", where *x* is the atomic percentage of copper. The galvanic couples are named as *y*/*z* where *y* and *z* are the atomic percentages of copper in the anode and cathode, respectively.

3. Results and discussion

Fig. 1 shows a transmission electron micrograph of the Al–1.8 at.% Cu alloy. The deposited alloy has a relatively uniform thickness, about 400 nm, and adheres to the substrate. The alloy is also uniform in composition and has a nano-crystalline structure. Other than for the layer thickness which was dependent on the copper content, although all the alloys were deposited for a similar time (50 min.), similar features were evident for all the alloys. Concerning the effect of copper, the layer thickness increased slightly, from 400 to 500 nm, with increase of copper content from 0 to 50% and then more rapidly for higher copper contents, reaching 900 nm for pure copper. This is explained by the increased sputtering rate of copper compared with aluminium.

According to the equilibrium phase diagram, different phases can be present in Al–Cu alloys, namely (with increasing copper content): α-Al, θ-Al_2Cu, η_2-AlCu, ξ_2-Al_9Cu_{12}, δ, γ_2-Al_4Cu_9, α_2, α-Cu. In the selected samples, with copper contents in the 0–42 at.% Cu range (corresponding to the samples listed in Table 1), only α, θ and η_2 phases were detected. Monophased or biphased ($\alpha + \theta$ or $\theta + \eta_2$) alloys were evident. The proportion of the different metallurgical phases was approximately verified for four Al–Cu model alloys by examining at least 20 diffraction patterns from different locations on the specimen and by calculating the proportion of each phase. This proportion is representative of the volume percentage of the phases and is compared in Table 1 with the volume proportion determined from the equilibrium phase diagram using densities of 2.70, 4.33 and 4.46 for α-Al, θ-Al_2Cu and η_2-AlCu, respectively. Good agreement is evident between the calculated proportions and the proportions estimated from the diffraction patterns. Thus, the structure of the alloys deposited by magnetron sputtering is in good agreement with the equilibrium phase diagram.

Table 1
Theoretical and measured volume proportions of the different metallurgical phases present in ($\alpha + \theta$) and ($\theta + \eta_2$)-containing Al–Cu alloys

Alloy	vol.%[a]			% of diffraction patterns		
	α-Al	θ	η_2	α-Al	θ	η_2
Al–0.2Cu	99.5	0.5	–			
A1–1.8Cu	95.1	4.9	–			
Al–2.5Cu	93.2	6.8	–			
Al–3Cu	91.8	8.2	–			
Al–7Cu	80.6	19.4	–			
Al–22Cu	35.7	64.3	–	30	70	
Al–33Cu	–	100	–		95	5
Al–35Cu	–	87	13		90	10
Al–42Cu	–	44	56		50	50

[a] Calculated from the equilibrium phase diagram.

Fig. 2 shows the influence of the copper content on the open circuit potential (OCP) of the Al–Cu alloys obtained after immersion for 1 h in sulphate solution. A significant and rapid increase of the OCP with increase of copper content was observed in the 0–7 at.% Cu range, followed by a slower increase with increase of copper content from 7 to 33 at.% Cu; at 33 at.% copper, only the θ phase is present in the alloy. For copper contents in the 33–100 at.% Cu range, a fast increase of OCP over a narrow copper content range was followed by a slow increase of the OCP to that of pure copper. The variation of

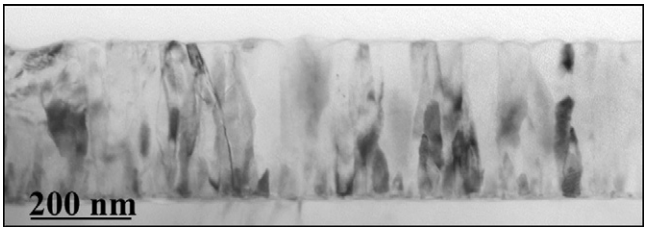

Fig. 1. Transmission electron micrograph of the Al–1.8 at.% Cu alloy deposited by magnetron sputtering.

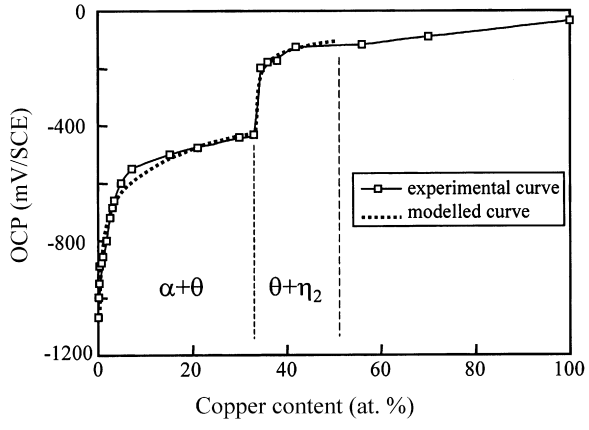

Fig. 2. Influence of the copper content on the open circuit potential (OCP) of Al–Cu alloys after immersion of 1 h in 0.1 M Na_2SO_4 solution.

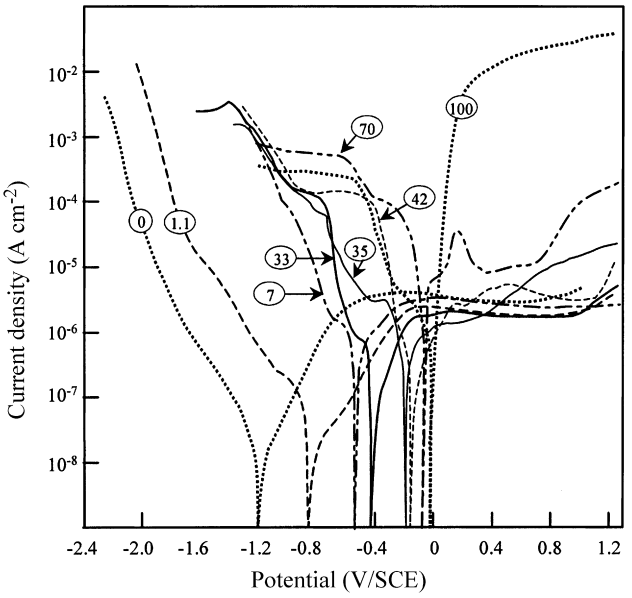

Fig. 3. Potentiodynamic polarization curves of different Al–Cu alloys in 0.1 M Na_2SO_4 solution (potential scan rate: 1 V/h). The number on each curve represents the atomic percentage of copper in the alloy.

OCP with copper content can be explained by comparing the potentiokinetic polarization curves of the different alloys. Fig. 3 presents some examples of the polarization behaviour obtained by scanning the potential from the OCP towards the anodic or cathodic direction at a rate of 1 V/h. It was observed that for all the alloys, except for the highest copper content alloys, i.e. pure copper and Al–70Cu, the anodic part of the curves is characterized by the presence of a passivity plateau situated in the $1–3 \times 10^{-6}$ A cm^{-2} range. Conversely, the cathodic parts of the curves depended on the copper content of the alloy. Fig. 4(a) and (b) shows that the potentiodynamic polarization curves of the α phase (α pure Al) and the θ phase (Al–33Cu) can be explained as the addition of an anodic curve corresponding to the passivity plateau and a cathodic curve comprised of the oxygen reduction curve with a diffusion plateau at a value of about 3×10^{-6} A cm^{-2} and the water reduction curve. From the schematic partial curves of Fig. 4(a) and (b) (dotted curves), it is evident that the oxygen plateaus for the α and θ phases have similar values. However, comparing the activation polarization regions of this reaction, it appears that, at a given potential, the rate of the oxygen reduction is much higher on θ phase than on α phase.

In (α + θ)-containing alloys, i.e. alloys with a copper content in the 0–33 at.% Cu range, the current density i_c of oxygen reduction depends on the volume proportions (S_α and S_θ) according to:

$$i_c = S_\alpha i_c(\alpha) + S_\theta i_c(\theta) \quad (1)$$

If the copper content is higher than a few at.%, the current on the α phase is negligible compared with the current on the θ phase, and then:

$$i_c = S_\theta i_c(\theta) \quad (2)$$

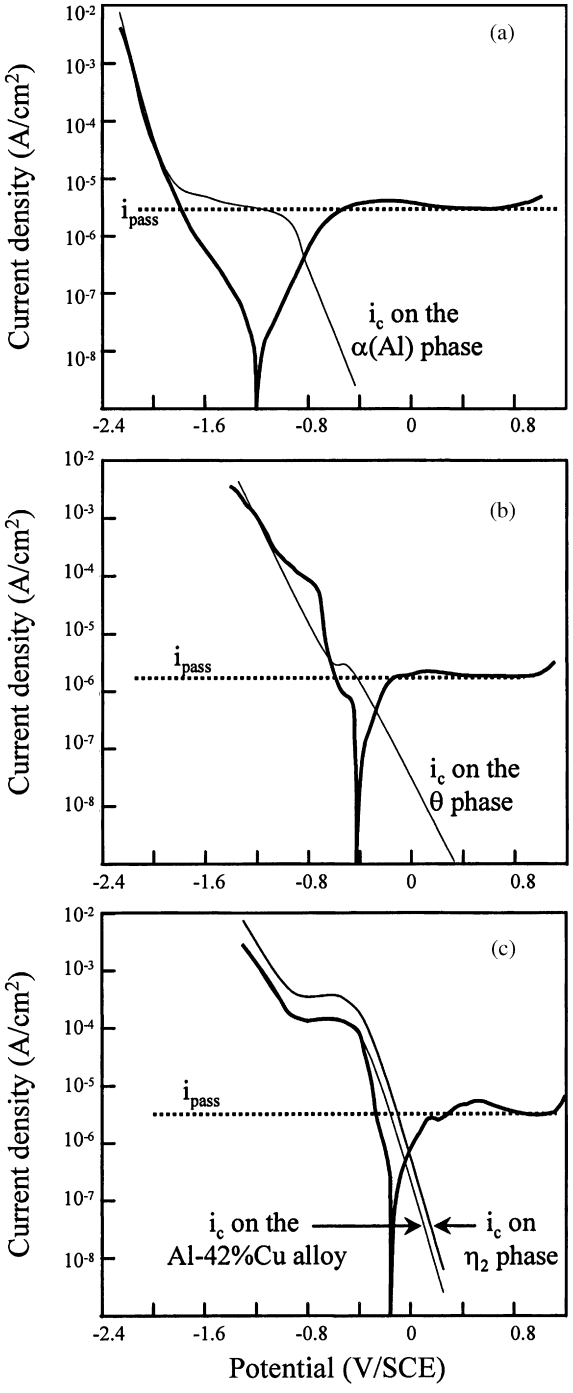

Fig. 4. Potentiodynamic polarization curves and anodic and cathodic partial curves on (a) pure Al, i.e. α phase, (b) on Al–33Cu, i.e. θ phase and (c) on Al–42Cu containing 56 vol.% η_2 phase.

Further, the cathodic current depends on the potential according to the Tafel equation:

$$E = E_0 + b_c \log\left[\frac{i_c}{i_c^0}\right] \quad (3)$$

Combining Eq. (2) and Eq. (3) gives:

$$E = E_0 + b_c \log\left[\frac{S_\theta i_c(\theta)}{S_\theta i_c^0(\theta)}\right] \quad (4)$$

The corrosion potential, E_{corr}, is obtained when $S_\theta i_c(\theta)$ is equal to the passive current, i_{pass}:

$$E_{corr} = E_0 + b_c \log\left[\frac{i_{pass}}{S_\theta i_c^0(\theta)}\right] \quad (5)$$

The current density $i_c^0(\theta)$ is a constant and the passive current can also be considered to be constant since it is similar for all the $(\alpha+\theta)$-containing alloys. Consequently, the corrosion potential is dependent only on the proportion of the θ phase according to the relation:

$$E_{corr} = k - b_c \log[S_\theta] \quad (6)$$

Finally, since the proportion of the θ phase varies with the atomic percentage of copper according to the approximate relation:

$$S_\theta = 3\,\text{at.\%}\ \text{Cu} \quad (7)$$

The corrosion potential varies logarithmically with the atomic percentage of copper:

$$E_{corr} = k - b_c \log[3\,\text{at.\%}\ \text{Cu}] \quad (8)$$

Fig. 2 shows that the OCP varies according to such an expression between 0 and 33 at.% Cu.

Calculations were performed to determine the values of the parameters of Eq. (8), leading to the best fit with the experimental data. A value of −240 mV was obtained for the Tafel slope, which is a plausible value for the oxygen reduction reaction on the θ phase.

For $(\theta+\eta_2)$-containing alloys (between 33 and 50 at.% Cu), a logarithmic variation of the OCP with the copper content was also observed (Fig. 2). A similar explanation is also valid for these alloys since the kinetics of oxygen reduction on the η_2 phase are much higher than on the θ phase (Fig. 4(b) and (c)). In this case, the best fit between the experimental data and the model was obtained with a value of −95 mV for the Tafel slope for the oxygen reduction reaction on η_2 phase.

For $(\eta_2+\xi_2)$ or $(\xi_2+\delta)$-containing alloys, the previously established behaviour was not observed since the OCP increased slightly between 50 and 100 at.% Cu. This observation results from the similar rate of oxygen reduction on the highest Cu-containing phases (η_2, ξ_2, δ, γ_2,...) (Fig. 3).

3.1. Galvanic coupling between $(\alpha+\theta)$-containing alloys

Fig. 5 shows the galvanic coupling current recorded for a protracted time (60,000 s) of immersion for the 3/33 couple. In this couple, the alloy of the highest copper content clearly acted as the cathode. The current increased from zero at the beginning over about 6000 s and finally decreased. At 60,000 s, a current of 0.3 μA was recorded, i.e. a value lower than the passive current (Fig. 3). Fig. 6 shows the 7200 first seconds of galvanic current–time curves recorded for different couples between alloys containing both α and θ phases and alloys containing both α and θ phases or largely the θ phase (Al–33Cu). It is evident that the higher the copper content of the anode, the higher the maximum current reached during coupling. Further,

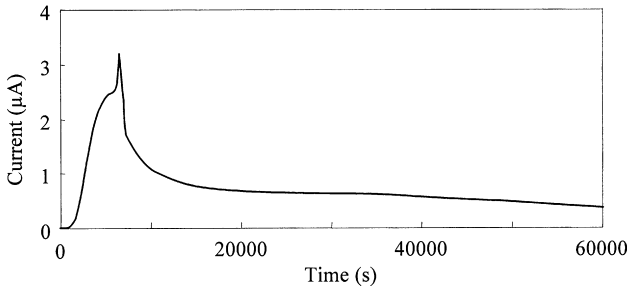

Fig. 5. Variation of galvanic coupling current with time for the 3/33 couple in 0.1 M Na_2SO_4 solution.

it appears that for couples with an anode containing a high copper content (3–22 at.%) the curves have a similar shape to that for couples with an anode of low copper content (0.2–2.5 at.%), other than for the presence of a small peak in current which is superimposed on the curve. This peak appeared at earlier immersion times when the copper content of the anode was increased.

In all the galvanic couples, both α and θ phases are present in the anode and cathode. It can be assumed that the α phase reveals anodic behaviour both at the anode and cathode with similar anodic current densities, i_a. Further, the θ phases in the anode and cathode have cathodic behaviour (oxygen reduction) of similar cathodic current densities, i_c. The surface areas of the α phase and θ phase in both electrodes can be deduced from the volume proportions given in Table 1. Using the notation indicated in Fig. 7, the galvanic coupling current measured during the tests, I_{meas}, is equal to $(I_{c2}-I_{a2})$ or $(I_{a1}-I_{c1})$. Then, the anodic current density i_a equals:

$$i_a = I_{meas}\left(\frac{S_{c1}+S_{c2}}{S_{a1}S_{c2}-S_{a2}S_{c1}}\right) \quad (9)$$

The anodic current density, i_a, is thus proportional to the measured galvanic coupling current. The proportionality factor depends on the volume fractions of the α and θ phases in the anode and cathode. Fig. 8 shows the variation of anodic current density with time for different couples. The greater the copper content of the anode, i.e. the greater the proportion of the θ phase, the faster the initial increase of the anodic current and the higher

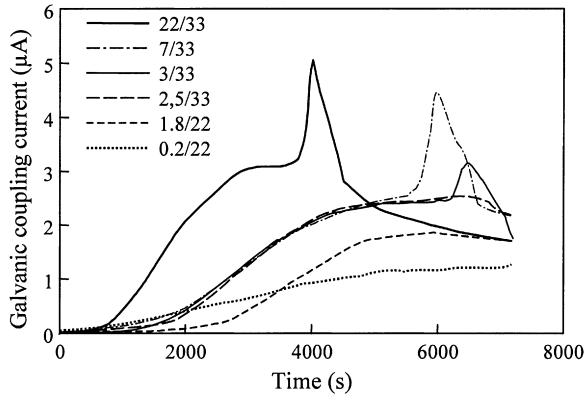

Fig. 6. Variation of galvanic coupling current with time for couples of Al–Cu alloys with copper content from 0.2 to 33 at.% Cu.

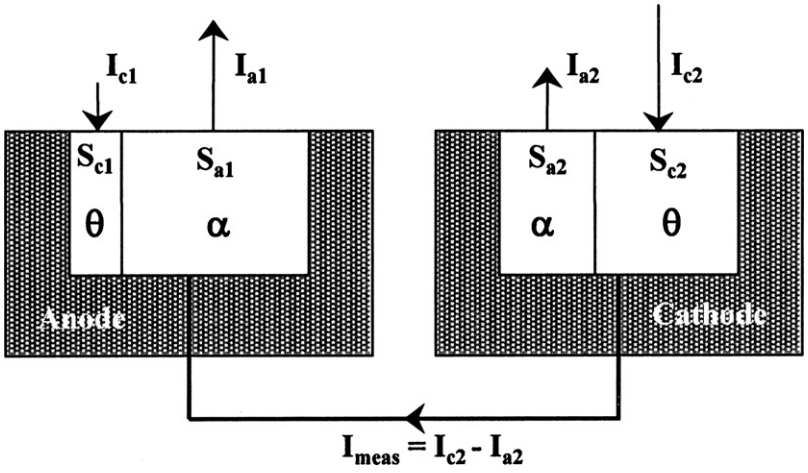

Fig. 7. Schematic representation of the electrochemical reactions occurring on a galvanic couple composed of two (α + θ)-containing alloys.

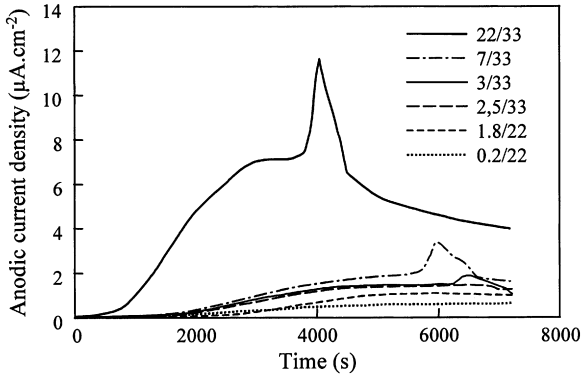

Fig. 8. Variation of anodic current density, i_a, with time for galvanic couples of Al–Cu alloys with copper content from 0.2 to 33 at.% Cu.

the value i_a^{max} of the maximum of i_a (independent of the small peak).

Fig. 9 shows that the maximum current density, i_a^{max}, is proportional to S_c/S_a, where $S_c = S_{c1} + S_{c2}$ and $S_a = S_{a1} + S_{a2}$. Since $i_a = i_c$ (S_c/S_a), then the slope of the regression line corresponds to the cathodic current density i_c. The cathodic current density corresponding to the maximum of the current measured during the galvanic coupling tests has then the same value for all the couples and equals 1.5 μA cm^{-2}. This value is close to that of the oxygen reduction plateau observed on the potentiodynamic polarization curve of the Al–33 at.% Cu alloy (containing only the θ phase) in a similar solution.

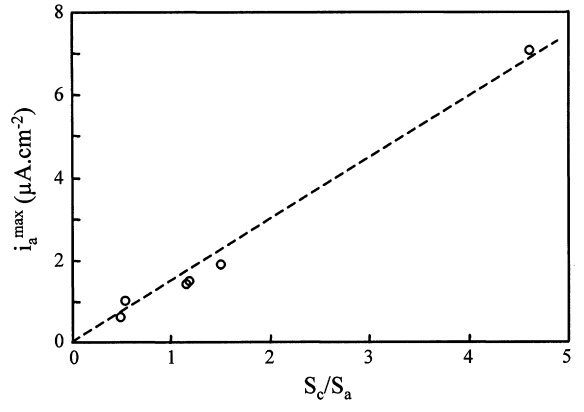

Fig. 9. Variation of the maximum anodic current density (i_a^{max}) with the θ to α surface area ratio.

For the galvanic coupling tests, the specimens were not treated after magnetron sputtering. Thus, an air-formed oxide film is present at the surface of the alloys. When the couple was immersed in sulphate solution, this film provided a good protection since the coupling current was initially zero. The current then increased showing that the film grown on the α phase was not stable in sulphate solution. Dissolution at air-formed film/electrolyte interface occurred followed by oxide film growth at the alloy/film interface. There was transformation of the air-formed film to a passive film, which was more stable due to the inhibitive effect of sulphate ions towards the α phase. This phenomenon can be partially explained by the galvanic coupling between α and θ phases. The kinetics of the oxidation reaction increased when the θ/α ratio increased. The increase of i_a was accompanied by an increase of i_c. However, when i_c reached the plateau value of 1.5 μA cm^{-2}, i.e. the limiting diffusion current for the cathodic reduction on θ phase, the kinetics of oxidation were at a maximum. For increased times, the transformation of air-formed film to passive film led to an improved protection, shown by the decrease of the current. The current values measured after immersion for 2 h are slightly lower than that observed for the passivity plateau on the potentiodynamic polarization curves of the individual model alloys. This showed that galvanic coupling led to an increase of the protective properties of the passive film formed on the α phase.

Thus, for Al–Cu alloys in sulphate solution, the galvanic coupling between the α phase and the θ phase is not found to be detrimental for the anodic α phase which remains in the passive state. The measured coupling current results from the transformation of the oxide film formed in air into an oxide film in sulphate solution. Fig. 10(a) confirms that the anode of a 1.8/21 couple is not attacked. Conversely, Fig. 10(b) and (c) reveals pits on the cathode. The pits are small holes at the centre of a large halo (30 μm in diameter in Fig. 10(c)) resulting probably

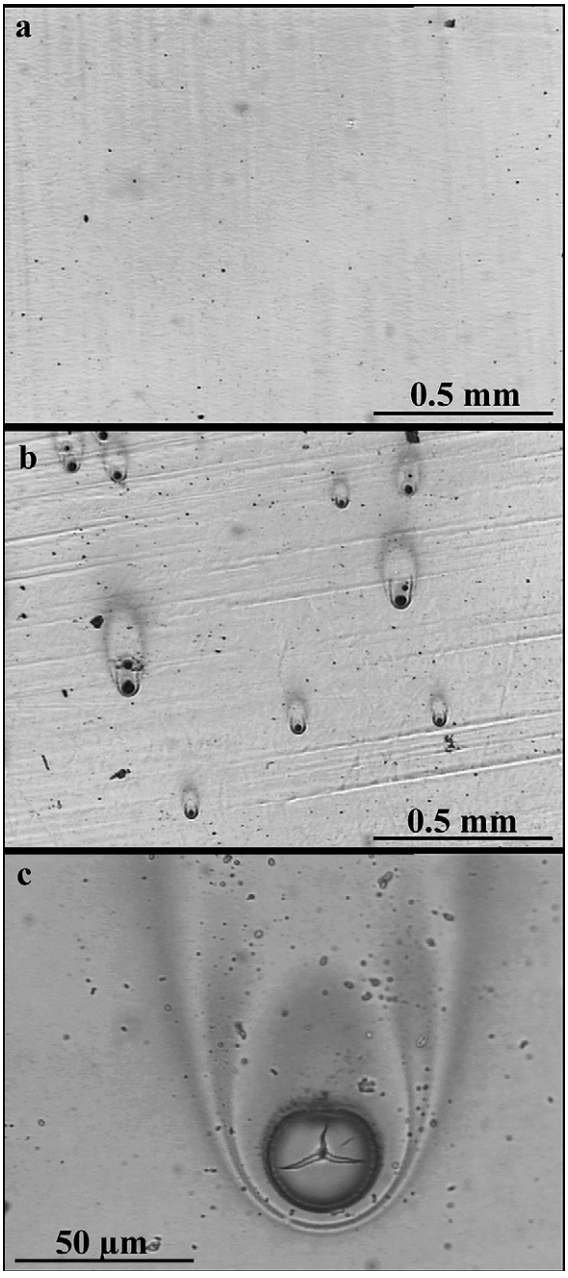

Fig. 10. Optical micrographs of the surface of (a) the Al–1.8Cu alloy and (b and c) the Al–22Cu alloy after galvanic coupling for 2 h in 0.1 M Na_2SO_4 solution.

of some corrosion products. Sulphate ions are known as aggressive species (more than chloride ions) towards copper and copper alloys and induce such pits on these materials [9,10]. The pits formed on the Cu-rich θ phase of the Al–21Cu sample, and were absent on the Al–1.8Cu alloy because of the very low proportion of the θ phase. Further pits were more numerous when the Al–33Cu alloy was coupled to an anode of lower copper content. Similarly, pits were more numerous on the Al–33Cu alloy than on the Al–22Cu alloy coupled to the same anode. These observations result from the pitting sites being more numerous on the cathode when the difference in copper contents between the anode and the cathode is more significant. Here, the Cu-rich phase is more susceptible to pitting when present at the cathode. The pits cannot propagate in depth more than 400 nm since they are stopped when they reach the substrate due to passivation of pure aluminium in sulphate solutions. They cannot also propagate laterally because of the columnar structure of grains (Fig. 1). In these conditions, the anodic current generated by pitting is very low and has negligible influence on the net measured current.

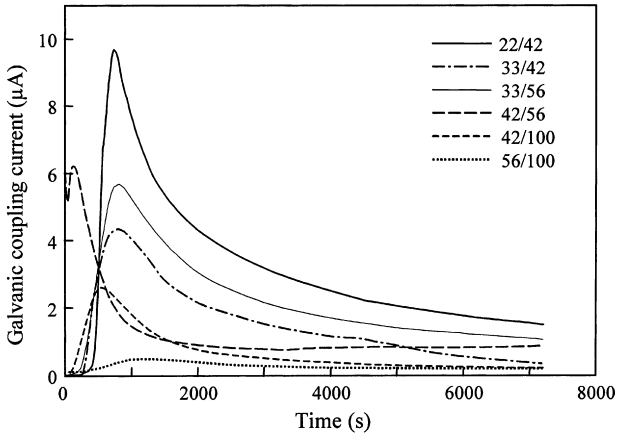

Fig. 11. Variation of galvanic coupling current with time for couples of Al–Cu alloys with high copper content.

These results are in good correlation with those observed in commercial alloys for which copper-rich particles (Al_2Cu, i.e. θ phase or Al_2CuMg, i.e. S phase) are known to be preferential sites for pitting and can also be helpful to understand the corrosion behaviour of coated alloys [15].

3.2. Galvanic coupling between high Cu-containing alloys

Fig. 11 shows the galvanic coupling current with time for couples of Al–Cu alloys with high copper contents. Curves similar to those for low copper content alloys were observed, although the maximum current is obtained at reduced times for all the couples. The measured currents are low and, after 2 h of coupling, their values are once more in the passive range. For high copper content alloys, the galvanic coupling does not promote corrosion of the more anodic phases.

Calculations were performed for the 22/42 couple to understand further the corrosion behaviour of the θ phase. For this couple, the anode (Al–22Cu alloy) is composed of 35.7 vol.% α and 64.3 vol.% θ, while the cathode (Al–42Cu alloy) is composed of 56 vol.% η_2 and 44 vol.% θ. For this couple, it is assumed that the α phase reveals anodic behaviour while η_2 has cathodic behaviour. For θ phase, it is more difficult to select between anodic or cathodic behaviour.

For a first hypothesis, it is assumed that the θ phase reveals anodic behaviour on both the anode and the cathode. Then, the following relations can be considered, taking into account the notations given in Fig. 12(a):

$$I_{\text{meas}} = I_c(\eta_2) - I_a^2(\theta) = I_a(\alpha) + I_a^1(\theta)$$

$$I_{\text{meas}} = S_{\eta_2} i_c(\eta_2) - S_{\theta_2} i_a(\theta) = S_\alpha i_a(\alpha) + S_{\theta_1} i_a(\theta)$$

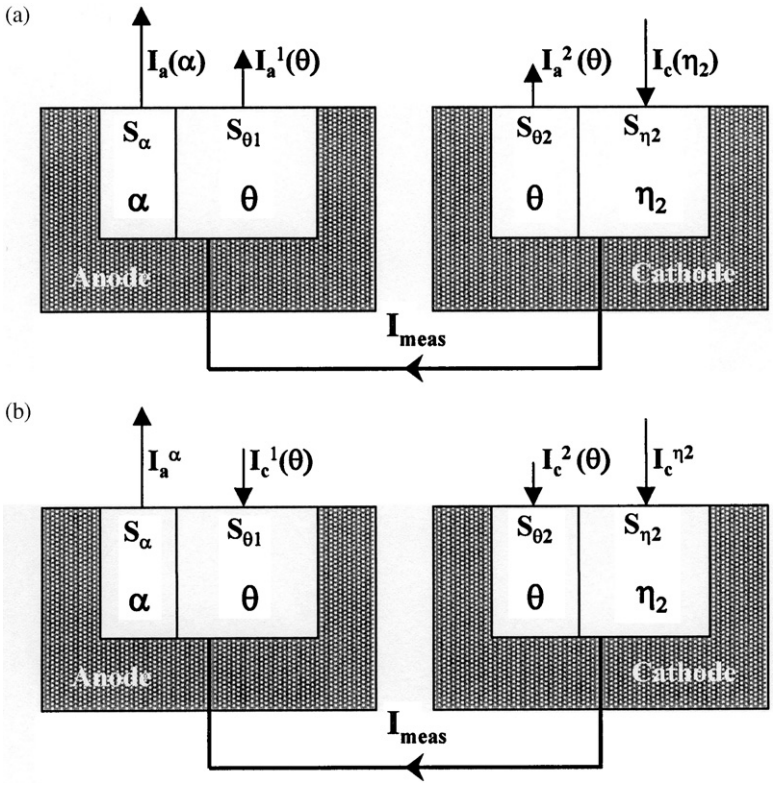

Fig. 12. Schematic representation of the electrochemical reactions occurring on a galvanic couple composed of a (α + θ)-containing alloy and a (θ + η_2)-containing alloy (a) in the case of anodic behaviour of the θ phase and (b) in the case of cathodic behaviour of the θ phase.

For the maximum current measured for the couple 22/42, i.e. 10 μA (Fig. 11), and for a given value of $i_c(\eta_2)$, it is possible to calculate the value of the anodic current densities on the α and θ phases, i.e. $i_a(\alpha)$ and $i_a(\theta)$. Fig. 4(c) shows that the maximum value of $i_c(\eta_2)$, i.e. the diffusion plateau value of the current density for the oxygen reduction on the η_2 phase was about 200 μA cm^{-2}. Using this value for $i_c(\eta_2)$, calculation led to values of 243 μA cm^{-2} and −424 μA cm^{-2} for respectively $i_a(\theta)$ and $i_a(\alpha)$. A negative value for $i_a(\alpha)$ signifies that the α phase should have a cathodic behaviour which is opposite to the hypothesis. Further calculations showed that positive values can be obtained simultaneously for $i_a(\theta)$ and $i_a(\alpha)$ only if the value of $i_c(\eta_2)$ is in a narrow range (between 0.9 and 1.5 × 10^{-5} A cm^{-2}). In this case, the corresponding ranges for $i_a(\theta)$ and $i_a(\alpha)$ are 7.7–0.09 mA cm^{-2} and 0.09–13.8 mA cm^{-2}, respectively. All these current ranges are compatible with a potential of the galvanic couple close to the corrosion potential of the Al–42Cu alloy.

The second hypothesis assumed that the θ phase reveals cathodic behaviour on both the anode and the cathode. Then, the following relations can be considered, taking into account the notations given in Fig. 12(b):

$$I_{meas} = I_c^2(\theta) + I_c(\eta_2) = I_a(\alpha) - I_c^1(\theta)$$

$$I_{meas} = S_{\theta_2} i_c(\theta) + S_{\eta_2} i_c(\eta_2) = S_\alpha i_a(\alpha) - S_{\theta_1} i_c(\theta)$$

If I_{meas} is equal to 10 μA, then $i_c(\eta_2)$ cannot be higher than I_{meas}/S_η, i.e. 11.4 μA cm^{-2}. According to Fig. 4, the potential of the couple must be higher than −0.2 V/SCE. In this potential range, the behaviour of the θ phase is predominantly anodic and then in opposition to the hypothesis.

As a conclusion, it appears that in galvanic couple containing the three phases α, θ and η_2, only the η_2 phase has cathodic behaviour and the potential of the couple is close to the potential of the η_2 phase. This is in agreement with Fig. 2 showing that when two phases are in presence, the potential of the couple is close to the potential of the Cu-richer phase. This is also true when three phases are coupled.

For the alloys with a very high copper content, there were not significant differences between the OCP values (Fig. 2), and this led to very low galvanic currents during coupling of such alloys.

Fig. 13 shows optical micrographs of the anode and cathode of a 33/42 couple. Similar observations to those for couples of low copper content can be made: the Al–33Cu anode shows only a few pits, whereas the Al–42Cu cathode is highly pitted. Even if the Al–33Cu alloy is composed exclusively of the susceptible θ phase, the pits are less numerous than in the case where this alloy is coupled to a low copper content alloy. The Al–42Cu alloy is composed of 56 vol.% η_2 and 44 vol.% θ. The surface of the 33/42 couple is then composed of about 3/4 of θ and 1/4 of η_2. The η_2 phase appears to be much more susceptible to pitting than the θ phase. This shows that the pitting susceptibility of the different phases in sulphate solutions greatly increases with copper content. Pitting of copper-rich phases led to the protection of phases containing less copper. This can be related to the behaviour of commer-

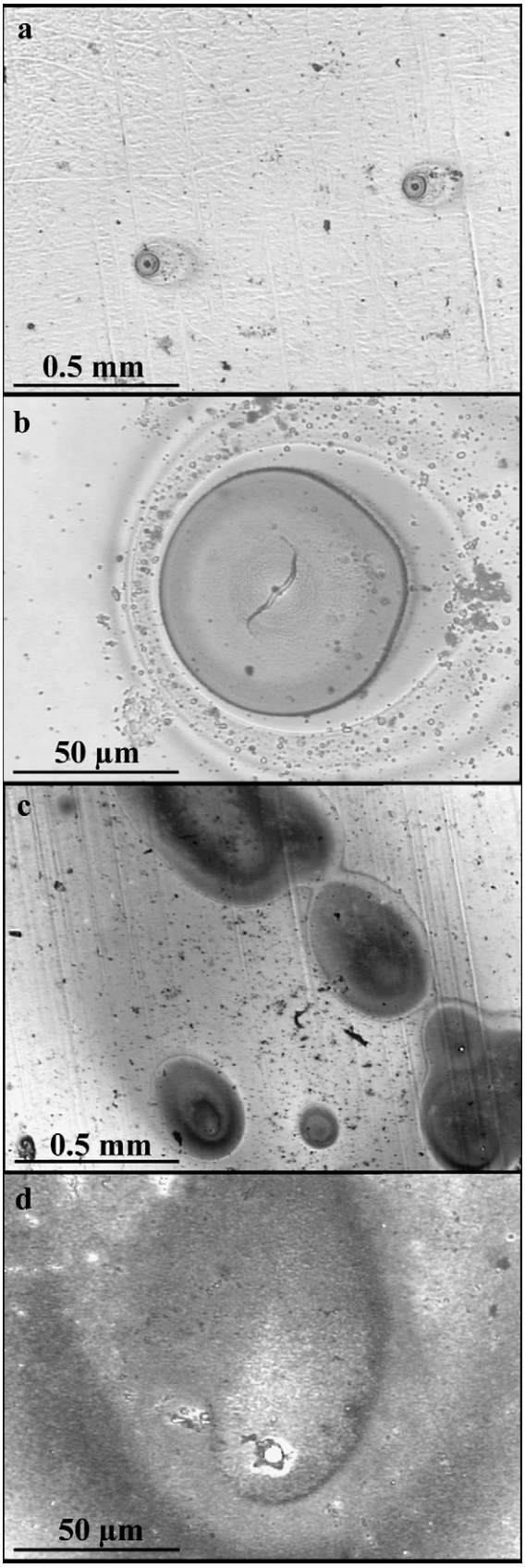

Fig. 13. Optical micrographs of the surface of (a and b) the Al–33Cu alloy and (c and d) the Al–42Cu alloy after galvanic coupling for 2 h in 0.1 M Na_2SO_4 solution.

cial alloys [6]. In a first step, pits form on θ or S phases while the matrix (α phase) remains passive. Pitting of the θ phase leads to the generation of copper species that can then form deposits of pure copper on the intermetallics and on the surrounding matrix. In a second step, pits form on the copper deposits due to galvanic coupling between pure copper and both α and θ phases: the θ phase stops dissolving while copper deposits on the matrix are corroded. Since the copper deposits correspond to thin films of copper on the matrix, pits rapidly cease to propagate; the matrix is exposed again to the electrolyte, but repassivates due to the inhibitive effect of sulphate ions towards the matrix. Thus, only micropits were observed on the copper deposits [3]. Then, the θ phase acts alternatively as an anode and as a cathode since it is alternatively coupled with the matrix (α phase) and with pure copper (copper deposits).

4. Conclusions

In 0.1 M Na_2SO_4 solution, galvanic coupling between Al–Cu alloys containing α and θ phases showed that the anodic α phase did not suffer corrosion and remained in the passive state. Conversely, the cathodic θ phase is susceptible to pitting induced by sulphate ions. The pitting susceptibility of the θ phase of the cathode increases when the difference of copper content between the anode and the cathode increased. It is also shown that the higher the copper contents of a phase, the greater its susceptibility to pitting in sulphate solutions.

References

[1] R.G. Buccheit, R.P. Grant, P.F. Hlava, B. Mckenzie, G.L. Zender, J. Electrochem. Soc. 144 (1997) 2621.
[2] V. Guillaumin, G. Mankowski, Corros. Sci. 41 (1999) 421.
[3] C. Blanc, B. Lavelle, G. Mankowski, Corros. Sci. 39 (1997) 495.
[4] A. Barbucci, G. Bruzzone, M. Delucchi, M. Panizza, G. Cerisola, Intermetallics 8 (2000) 305.
[5] C. Blanc, A. Freulon, M.C. Lafont, Y. Kihn, G. Mankowski, Corros. Sci. 48 (2006) 3838.
[6] C. Blanc, S. Gastaud, G. Mankowski, J. Electrochem. Soc. 150 (2003) B396.
[7] P. Schmutz, G.S. Frankel, J. Electrochem. Soc. 145 (1998) 2285.
[8] P. Schmutz, G.S. Frankel, J. Electrochem. Soc. 145 (1998) 2295.
[9] J.-P. Duthil, G. Mankowski, A. Giusti, Corros. Sci. 38 (1996) 1839.
[10] G. Mankowski, J.-P. Duthil, A. Giusti, Corros. Sci. 39 (1997) 27.
[11] Th. Suter, R.C. Alkire, J. Electrochem. Soc. 148 (2001) B36.
[12] M. Shao, Y. Fu, R. Hu, C. Lin, Mater. Sci. Eng. A 344 (2003) 323.
[13] Y. Liu, E.A. Sultan, E.V. Koroleva, P. Skeldon, G.E. Thompson, X. Zhou, K. Shimizu, H. Habazaki, Corros. Sci. 45 (2003) 789.
[14] S. Garcia-Vergara, P. Skeldon, G.E. Thompson, P. Bailey, T.C.Q. Noakes, H. Habazaki, K. Shimizu, Appl. Surf. Sci. 205 (2003) 121.
[15] M.W. Kendig, A.J. Davenport, H.S. Isaacs, Corros. Sci. 34 (1993) 41.